Supplementary Information

Clustered abasic lesions profoundly change the structure and stability of human telomeric G-quadruplexes

Kejnovská Iva[1], Bednářová Klára[1], Renčiuk Daniel[1], Dvořáková Zuzana[1], Školáková Petra[1], Trantírek Lukáš[2], Fiala Radovan[2], Vorlíčková Michaela[1]*, Sagi Janos[3]

[1] Institute of Biophysics, Czech Academy of Sciences, v.v.i., Královopolská 135, CZ-612 65 Brno, Czech Republic

[2] CEITEC—Central European Institute of Technology, Masaryk University, Kamenice 5, CZ-625 00 Brno, Czech Republic

[3] Rimstone Laboratory, RLI, Carlsbad, CA 92010, U.S.A

*To whom correspondence should be addressed: Tel.: +420 541517188; e-mail: mifi@ibp.cz

Table S1: The htel-22 d[$AG_3(TTAG_3)_3$] and htel-25 d[$TAG_3(TTAG_3)_3TT$] used in this paper

Name	5'-to-3' sequence
Substitutions in the htel-22:	
	1 7 13 19 22
wt-22	A GGG TT**A** GGG TT**A** GGG TT**A** GGG
	Loop substitutions
ap7	A GGG TT _ GGG TTA GGG TTA GGG
ap13	A GGG TTA GGG TT _ GGG TTA GGG
ap19	A GGG TTA GGG TTA GGG TT _ GGG
ap7,13	A GGG TT _ GGG TT _ GGG TTA GGG
ap7,19	A GGG TT _ GGG TTA GGG TT _ GGG
ap13,19	A GGG TTA GGG TT _ GGG TT _ GGG
ap17,18,19	A GGG TTA GGG TTA GGG _ _ _ GGG
ap7,13,19	A GGG TT _ GGG TT _ GGG TT _ GGG
Substitutions in the htel-25:	
	1 3,4,5 8 14 20 25
wt-25	TA **GGG** TT**A** GGG TT**A** GGG TT**A** GGG TT
	A/AP substitutions
ap8	TA GGG TT _ GGG TTA GGG TTA GGG TT
ap14	TA GGG TTA GGG TT _ GGG TTA GGG TT
ap20	TA GGG TTA GGG TTA GGG TT _ GGG TT
ap8,14,20	TA GGG TT _ GGG TT _ GGG TT _ GGG TT
	G/AP substitutions
ap3	TA _ GG TTA GGG TTA GGG TTA GGG TT
ap4	TA G _ G TTA GGG TTA GGG TTA GGG TT
ap5	TA GG _ TTA GGG TTA GGG TTA GGG TT
	(A+G)/AP substitutions
ap3,8	TA _ GG TT _ GGG TTA GGG TTA GGG TT
ap4,8	TA G _ G TT _ GGG TTA GGG TTA GGG TT
ap5,8	TA GG _ TT _ GGG TTA GGG TTA GGG TT
ap3,14	TA _ GG TTA GGG TT _ GGG TTA GGG TT
ap4,14	TA G _ G TTA GGG TT _ GGG TTA GGG TT
ap5,14	TA GG _ TTA GGG TT _ GGG TTA GGG TT
ap3,20	TA _ GG TTA GGG TTA GGG TT _ GGG TT
ap4,20	TA G _ G TTA GGG TTA GGG TT _ GGG TT
ap5,20	TA GG _ TTA GGG TTA GGG TT _ GGG TT
	clustered G/AP
ap3,4	TA _ _ G TTA GGG TTA GGG TTA GGG TT
ap3,4,5	TA _ _ _ TTA GGG TTA GGG TTA GGG TT
ap3,11	TA _ GG TTA GG _ TTA GGG TTA GGG TT
ap3,15	TA _ GG TTA GGG TTA _ GG TTA GGG TT
ap3,17	TA _ GG TTA GGG TTA GG _ TTA GGG TT
ap3,21	TA _ GG TTA GGG TTA GGG TTA _ GG TT
ap3,22	TA _ GG TTA GGG TTA GGG TTA G _ G TT
ap3,23	TA _ GG TTA GGG TTA GGG TTA GG _ TT
ap4,15	TA G _ G TTA GGG TTA _ GG TTA GGG TT
ap4,8,15	TA G _ G TT _ GGG TTA _ GG TTA GGG TT
ap4,11	TA G _ G TTA GG _ TTA GGG TTA GGG TT
ap4,11,20	TA G _ G TTA GG _ TTA GGG TT _ GGG TT
ap4,22	TA G _ G TTA GGG TTA GGG TTA G _ G TT
ap4,23	TA G _ G TTA GGG TTA GGG TTA GG _ TT
ap5,9	TA GG _ TTA _ GG TTA GGG TTA GGG TT
ap5,11	TA GG _ TTA GG _ TTA GGG TTA GGG TT
ap5,15	TA GG _ TTA GGG TTA _ GG TTA GGG TT
ap5,11,15	TA GG _ TTA GG _ TTA _ GG TTA GGG TT
ap5,21	TA GG _ TTA GGG TTA GGG TTA _ GG TT
ap5,20,21	TA GG _ TTA GGG TTA GGG TT _ _ GG TT
ap5,23	TA GG _ TTA GGG TTA GGG TTA GG _ TT

Table S2: Thermal stabilities of the htel-22 and htel-25 quadruplexes and their AP site modified analogs. Tm values were measured in 100 mM K^+ (10 mM K-phosphate + 85 mM KCl) and determined from the normalized 1-0 temperature dependences.

A)

htel-22		
name	**Tm [°C]**	**ΔTm [°C]**
wt-22	66.1	-
single A/AP		
ap7	66.0	-0.1
ap13	60.0	-6.1
ap19	66.5	0.4
double A/AP		
ap7,13	59.0	-7.1
ap7,19	60.0	-6.1
ap13,19	58.0	-8.1
triple A/AP		
ap17,18,19	67.5	1.4
ap7,13,19	68.2	2.1

B)

htel-25		
name	**Tm [°C]**	**ΔTm [°C]**
wt-25	62.0	-
single A/AP		
ap8	61.0	-1.0
ap14	55.8	-6.2
ap20	62.2	0.2
triple A/AP		
ap8,14,20	65.3	3.3
single G/AP		
ap3	46.5	-15.5
ap4	26.0	-36.0
ap5	39.5	-22.5
(A+G)/AP		
ap3,8	46.0	-16.0
ap4,8	30.0	-32.0
ap5,8	43.7	-18.3
ap3,14	42.2	-19.8
ap4,14	-	-
ap5,14	36.8	-25.2
ap3,20	40.8	-21.2
ap4,20	25.5	-36.5
ap5,20	36.2	-25.8

C)

htel-25		
name	**Tm [°C]**	**ΔTm [°C]**
clustered G/AP		
ap3,23	36.2	-25.8
ap3,15	35.8	-26.2
ap3,21	33.8	-28.2
ap3,11	32.5	-29.5
ap3,17	32.5	-29.5
ap3,22	25.0	-37.0
ap3,4,5	-	-
ap3,4	-	-
ap4,8,15	25.0	-37.0
ap4,15	23.5	-38.5
ap4,23	20.7	-41.3
ap4,11,20	18.2	-43.8
ap4,11	18.0	-44.0
ap4,22	-	-
ap5,23	35.2	-26.8
ap5,21	33.8	-28.2
ap5,9	32.0	-30.0
ap5,15	31.8	-30.2
ap5,11	31.0	-31.0
ap5,20,21	27.3	-34.7
ap5,11,15	27.0	-35.0

Table S3: Thermal stabilities of the htel-22 and htel-25 quadruplexes and their AP site modified analogs. Tm values were measured in 100 mM Na^+ (10 mM Na-phosphate + 85 mM NaCl) and determined from the normalized 1-0 temperature dependences.

A)

htel-22		
name	**Tm [°C]**	**ΔTm [°C]**
wt-22	57.2	-
single A/AP		
ap7	51.4	-5.8
ap13	51.0	-6.2
ap19	53.8	-3.4
triple A/AP		
ap7,13,19	38.4	-18.8

B)

htel-25		
name	**Tm [°C]**	**ΔTm [°C]**
wt-25	50.2	-
single A/AP		
ap8	50.1	-0.1
ap14	46.0	-4.2
ap20	52.0	1.8
triple A/AP		
ap8,14,20	33.00	-17.2
single G/AP		
ap3	41.0	-9.2
ap4	27.0	-23.2
ap5	39.4	-10.8
(A+G)/AP		
ap3,8	30.0	-20.2
ap4,8	19.8	-30.4
ap5,8	31.0	-19.2
ap3,14	32.4	-17.8
ap4,14	-	-
ap5,14	30.0	-20.2
ap3,20	33.7	-16.5
ap4,20	19.5	-30.7
ap5,20	34.5	-15.7

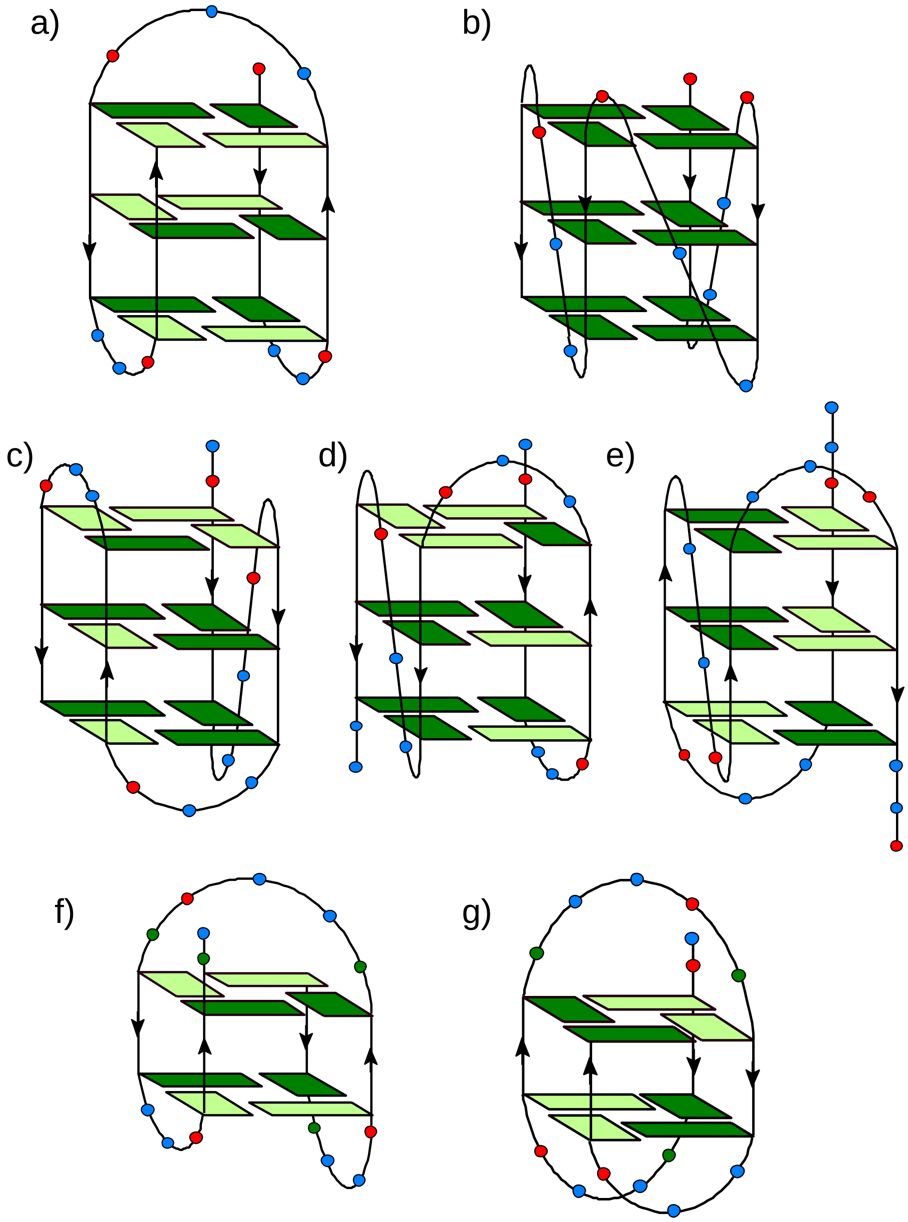

Figure S1: Various quadruplex folding topologies observed for human telomere sequences: (**a**) basket-type with edgewise-diagonal-edgewise loop configuration formed in Na^+ solution (1), (**b**) parallel topology with all loops in propeller-like configuration observed in crystal containing K^+ ions (2), **(c)** hybrid-1 (h-1) with propeller-like loop followed by two edgewise loops (3-6), and **(d)** hybrid-2 (h-2) two edgewise loops followed by propeller-like loop (6,7), both observed in K^+ solution, (**e**) (2 + 2) quadruplex with edgewise-propeller-edgewise loop configuration formed in Na^+ solution (8), (**f**) 2-tetrad basket quadruplex with edgewise-diagonal-edgewise loop formed in K^+ solution (9,10), and (**g**) 2-tetrad basket quadruplex with edgewise-diagonal-edgewise loop configuration but with a sugar-phosphate backbone running in the opposite direction, formed in K^+ solution and acidic pH (11). The deoxyadenosine and deoxythymidine residues are shown as red and blue circles, respectively. Tetrad deoxyguanosines in *anti*- and *syn*-conformation are represented by dark and light green rectangles, respectively.

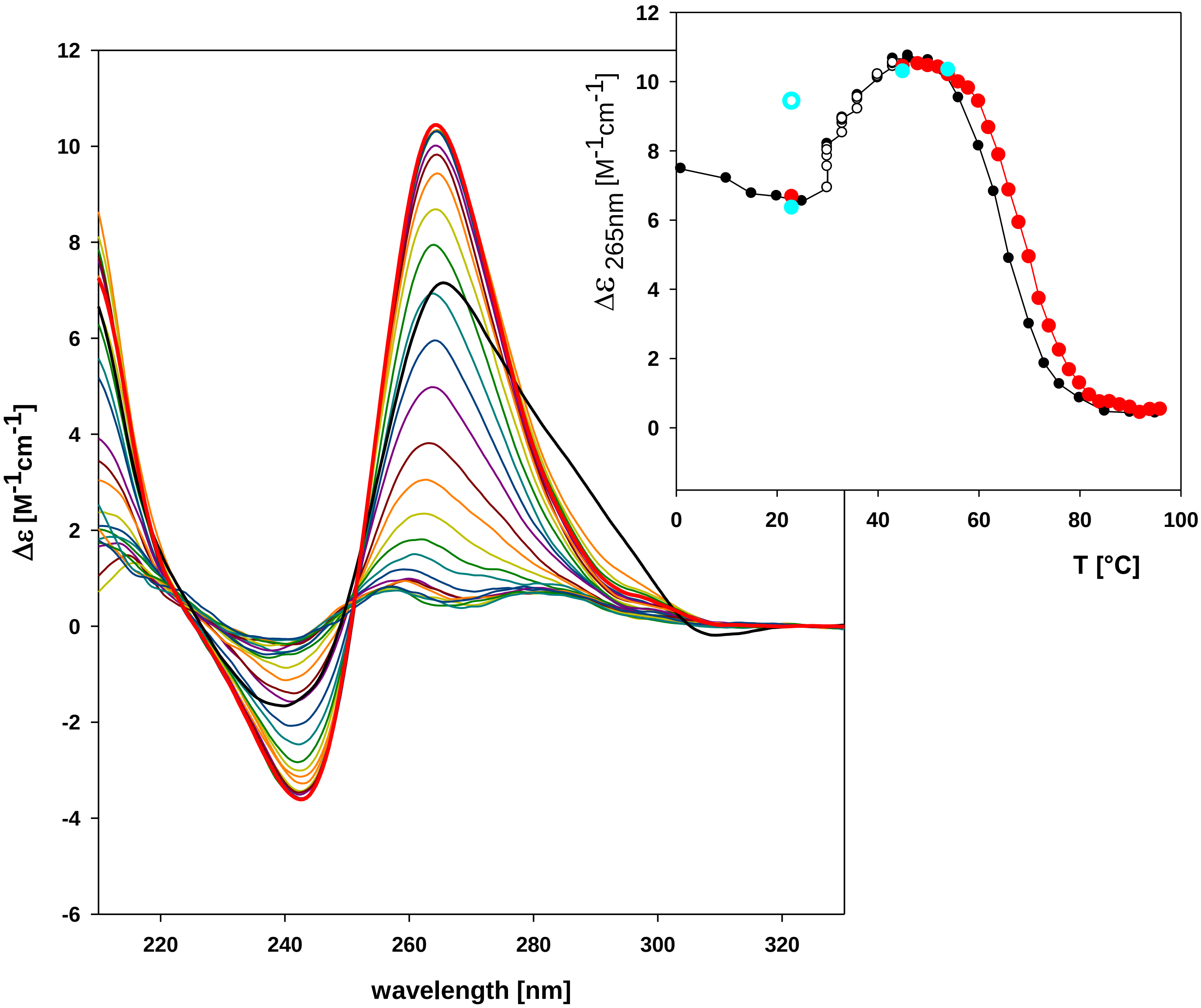

Figure S2: CD spectra and melting curves (insert) of ap7,13,19 htel-22 measured in 100 mM K^+. The black thick spectrum was taken at 23°C. Increasing the temperature resulted in time dependent formation of the parallel quadruplex at 45°C (red spectrum). Further increase in temperature up to 96°C led to quadruplex denaturation accompanied by decrease in CD amplitudes. Insert: Melting curves monitored at 265 nm in 60 mM K^+ (black circles, open circles correspond to non-equilibrium points), in 100 mM K^+ (red points). Starting from 45 °C to 96 °C melting took place; the cyan circles correspond to renaturation which was fast up to about 45 °C and very slow (24 hours – the open circle corresponds to non-equilibrium) returning to room temperature.

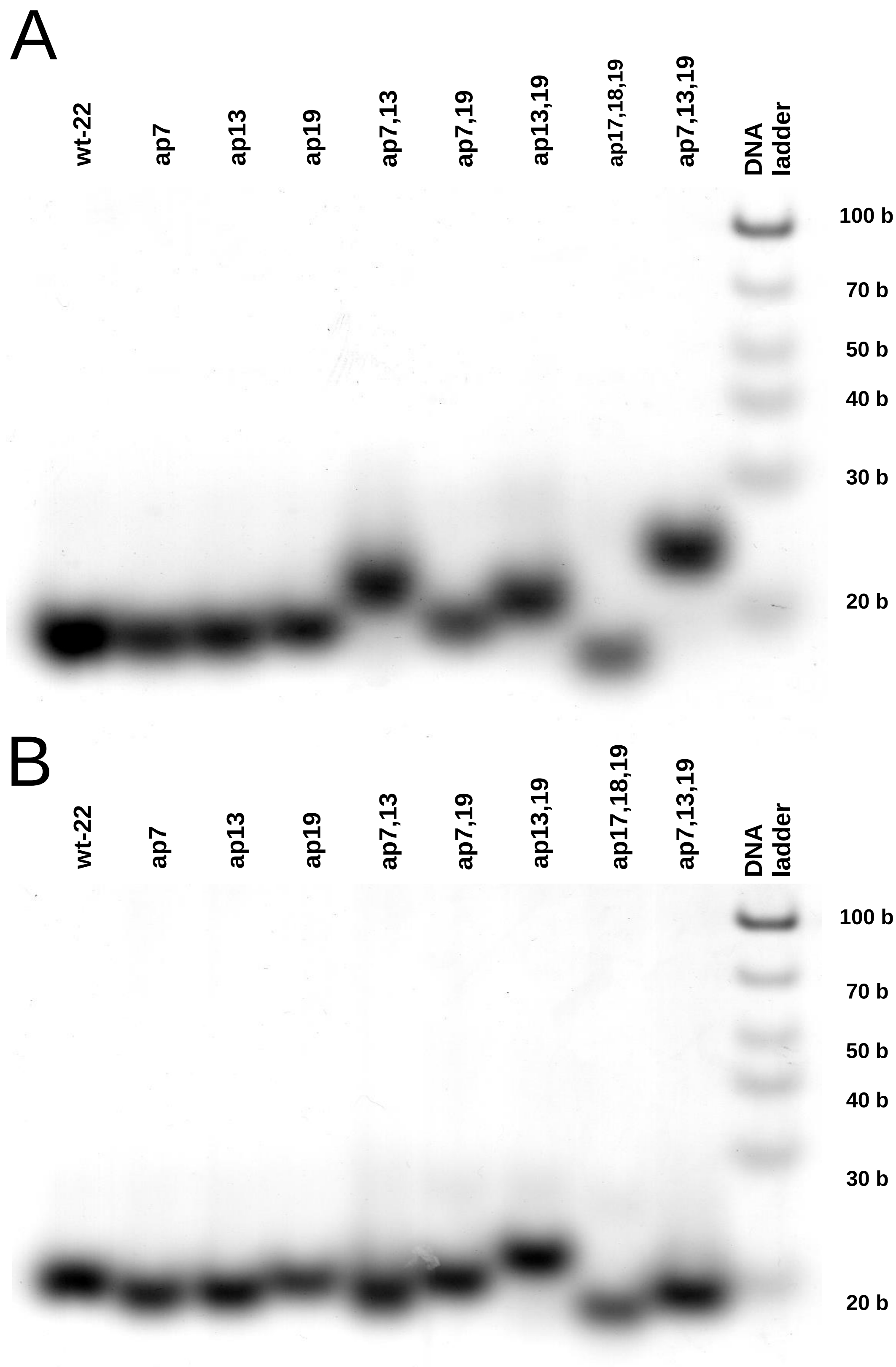

Figure S3: Native polyacrylamide gel electrophoresis of htel-22 analogs in (A): 10 mM K-phosphate buffer + 85 mM KCl, pH 7 (100 mM K^+) run at 35°C and (B): 10 mM Na-phosphate buffer + 85 mM NaCl, pH 7 (100 mM Na^+) run at 21°C.

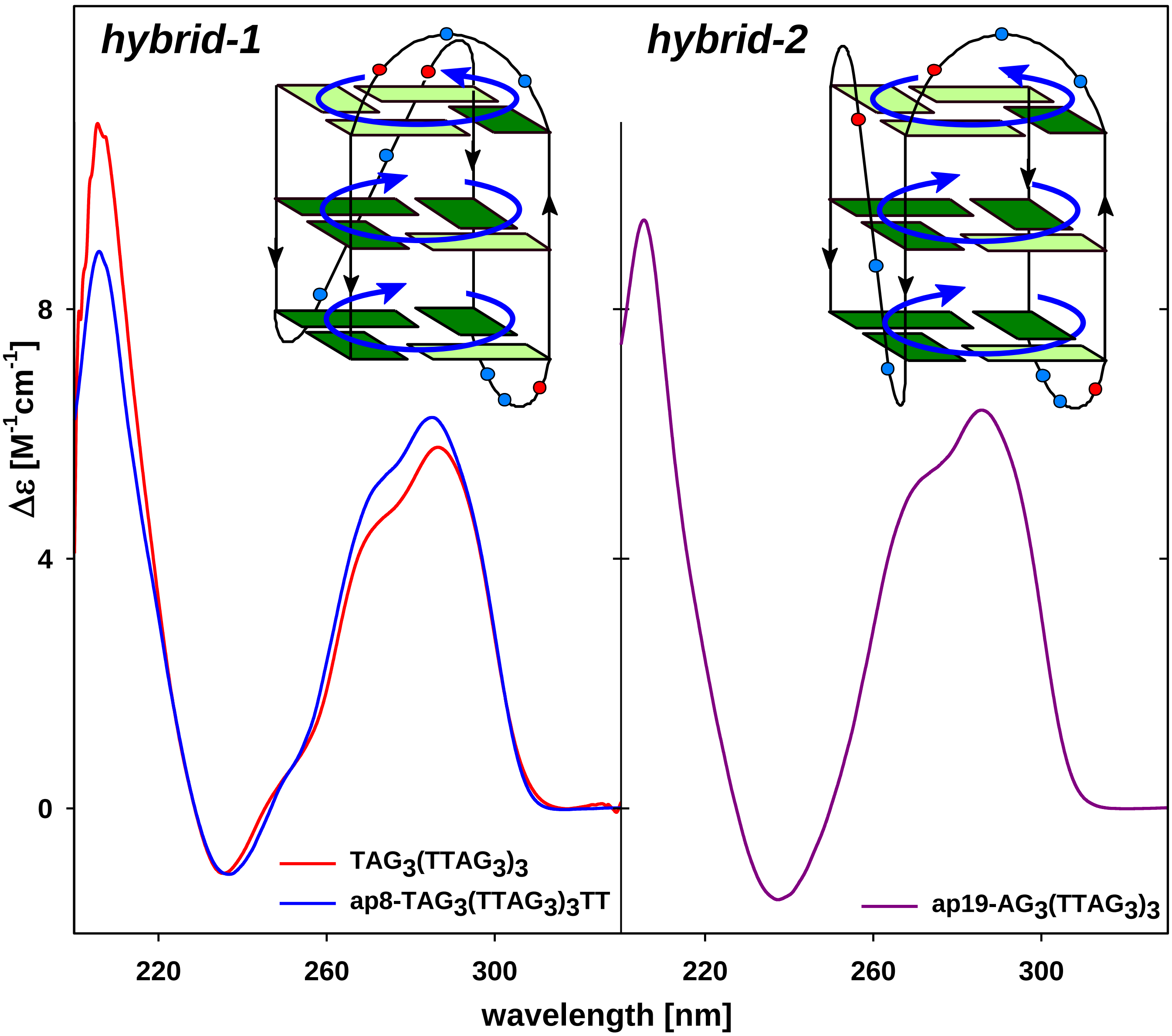

Figure S4: The same type of CD spectra provided by (left) htel-23 $TAG_3(TTAG_3)_3$ shown (12) to form h-1 quadruplex and of ap8 htel-25 $TAG_3(TTAG_3)_3TT$, and by (right) ap19 htel-22 shown (13) to form h-2 quadruplex. Inserts: The same orientation of quadruplex tetrads and *anti*/*syn* guanine glycosidic angles in the two hybrid structures drawn according to (12).

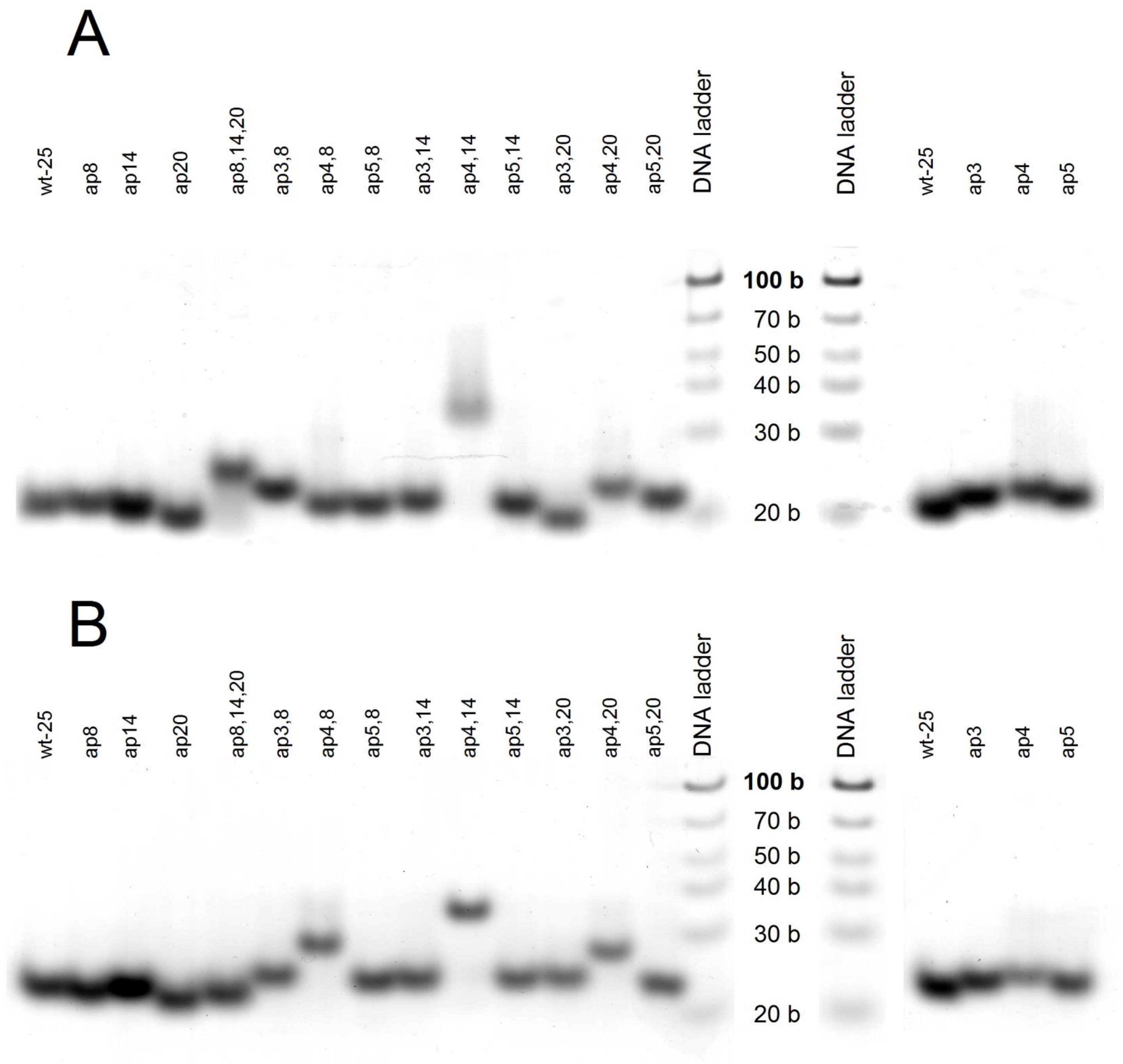

Figure S5: Native polyacrylamide gel electrophoresis of the htel-25 analogs in (A): 10 mM K-phosphate buffer + 85 mM KCl, pH 7 (100 mM K^+) and (B): 10 mM Na-phosphate buffer + 85 mM NaCl, pH 7 (100 mM Na^+), both run at 21°C.

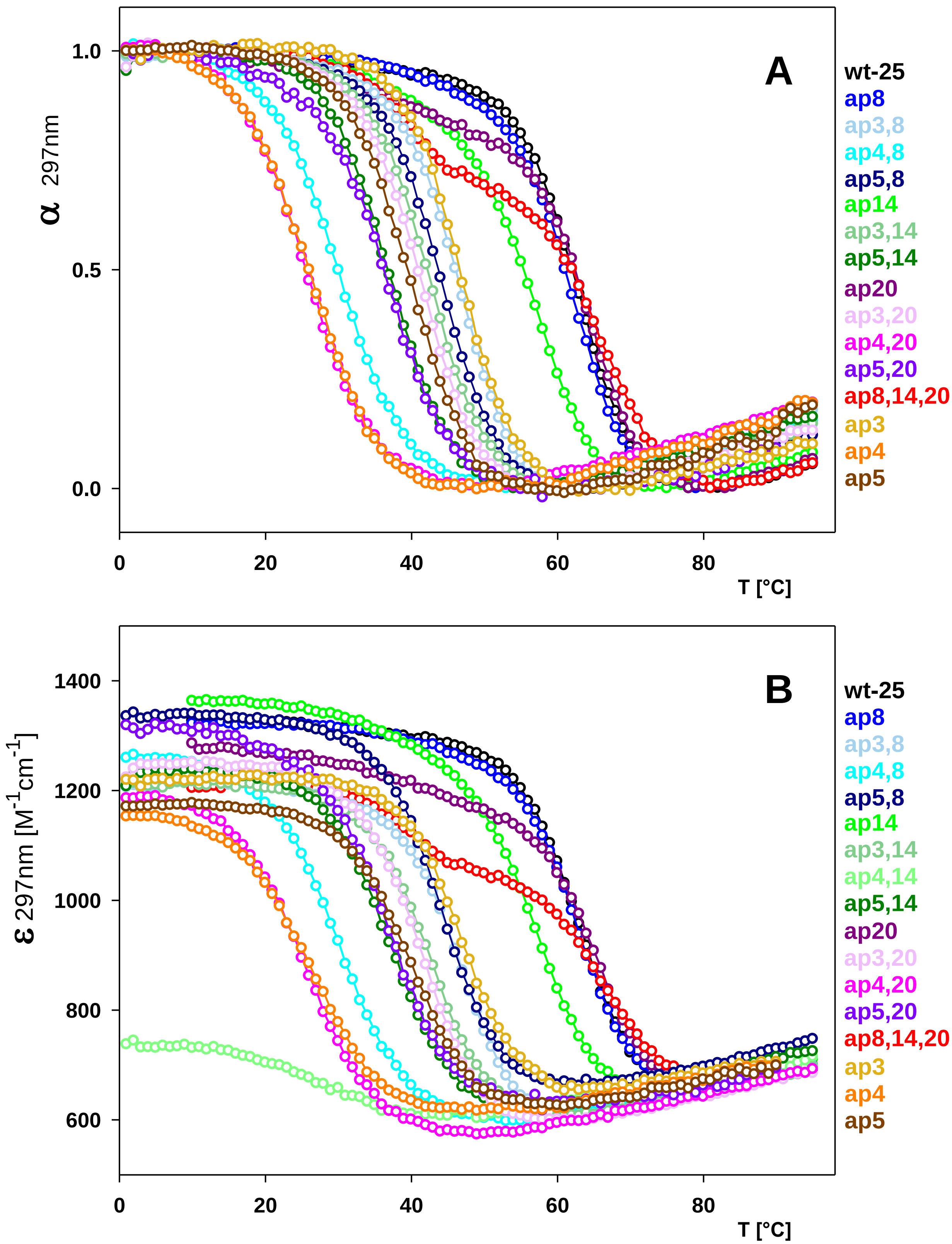

Figure S6: (A) Normalized melting profiles (1 stands for native, 0 for denatured state), and (B) melting profiles expressed in molar absorption of htel-25 analogs monitored by UV absorption at 297 nm measured in 100 mM K^+.

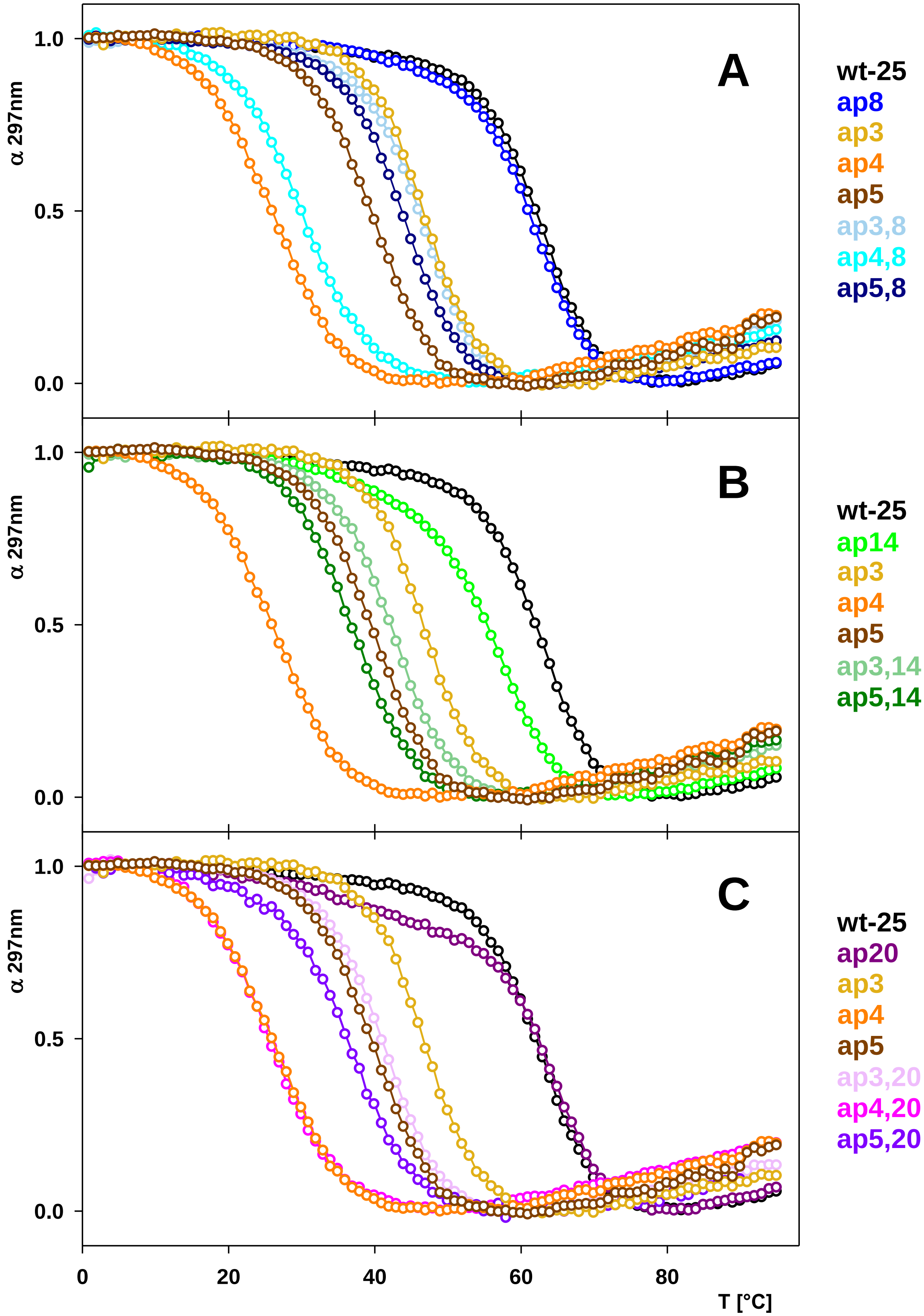

Figure S7: Normalized melting profiles of htel-25 wt and its (A+G)/AP analogs monitored by UV absorption at 297 nm measured in 100 mM K^+.

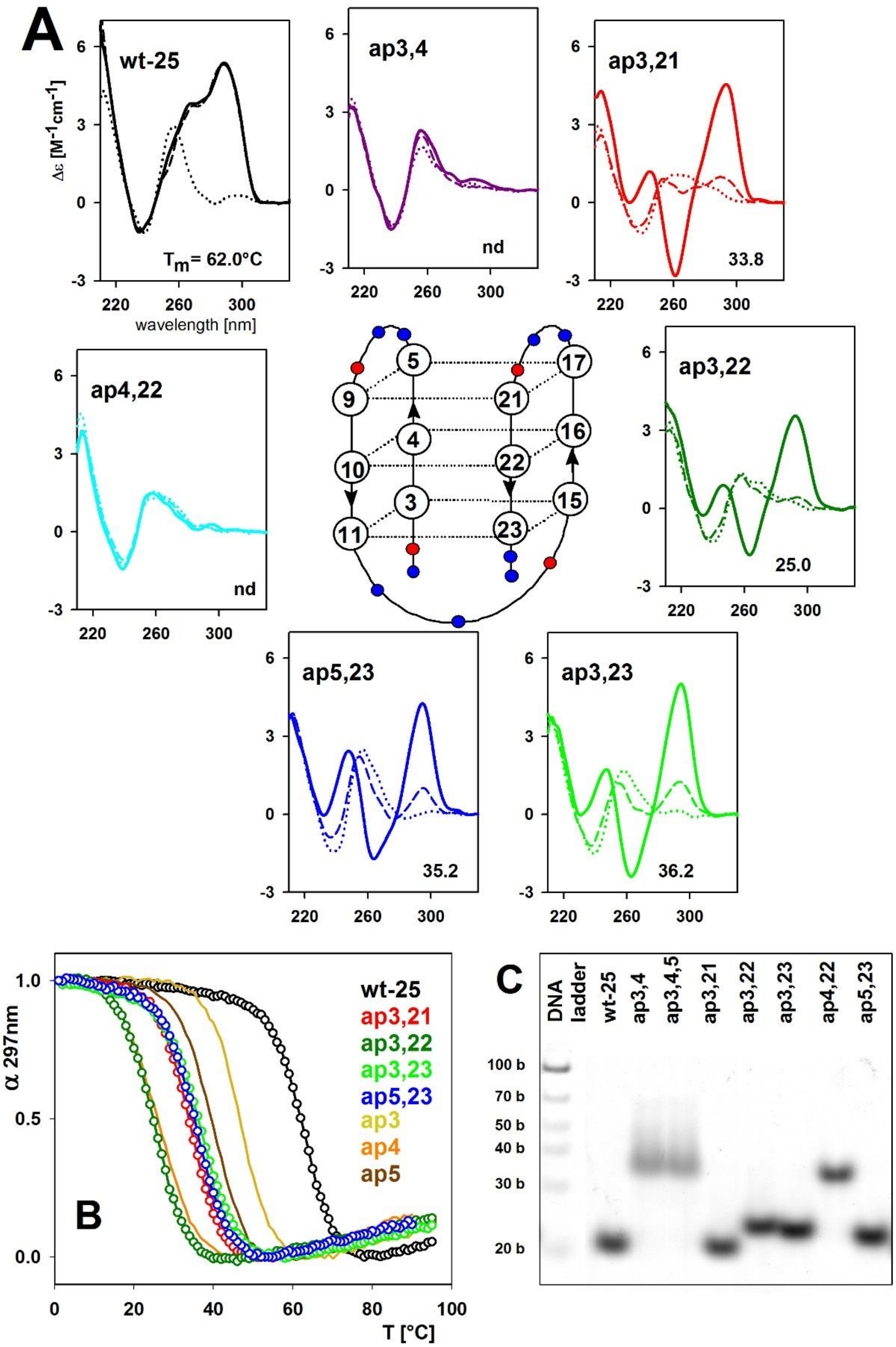

Figure S8: Double G/AP sites containing htel-25 analogs: (A) CD spectra in 1 mM sodium phosphate buffer with 0.3 mM EDTA, pH 7.2 (dotted lines), in 10 mM K-phosphate (dashed lines), and in K^+ added up to 100 mM (solid lines); the sketch of the quadruplex with numbering G positions (in the middle); (B) Normalized melting curves and (C) native PAGE. All measurements were undertaken in 100 mM K^+ at 21°C.

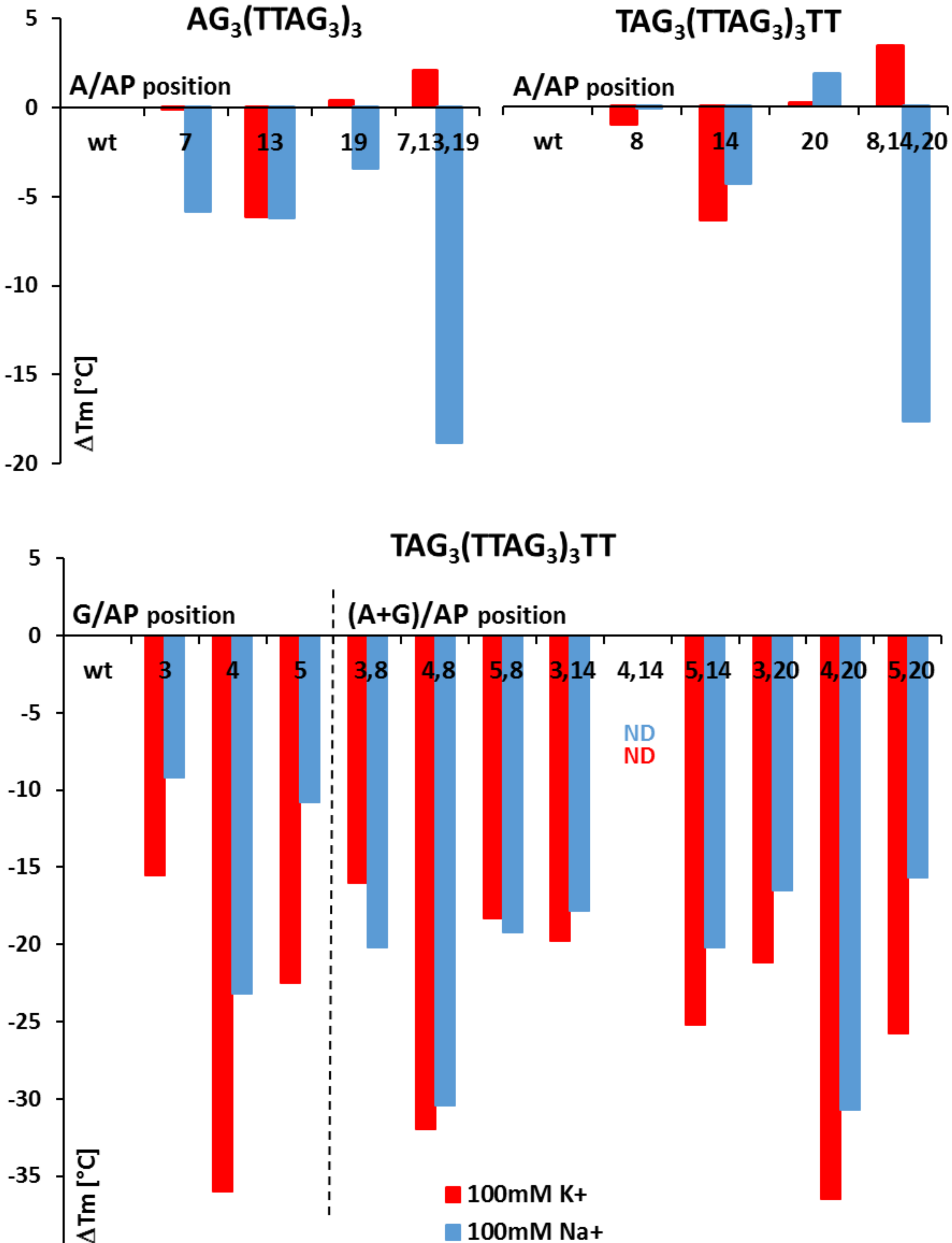

Figure S9: Column graphs of changes in Tm values caused by A/AP lesions (upper panels) in htel-22 (left) and htel-25 (right) analogs and by G/AP (left) and (A+G)/AP (right) lesions (bottom panels) in htel-25 analogs, compared to their wt´s, in 100 mM K^+ or 100 mM Na^+.

References

1. Wang,Y. and Patel,D.J. (1993) Solution structure of the human telomeric repeat d[AG3(T2AG3)3] G-tetraplex. *Structure*, **1**, 263–282.
2. Parkinson,G.N., Lee,M.P.H. and Neidle,S. (2002) Crystal structure of parallel quadruplexes from human telomeric DNA. *Nature*, **417**, 876–880.
3. Ambrus,A., Chen,D., Dai,J., Bialis,T., Jones,R.A. and Yang,D. (2006) Human telomeric sequence forms a hybrid-type intramolecular G-quadruplex structure with mixed parallel/antiparallel strands in potassium solution. *Nucleic Acids Res.*, **34**, 2723–2735.
4. Luu,K.N., Phan,A.T., Kuryavyi,V., Lacroix,L. and Patel,D.J. (2006) Structure of the human telomere in K+ solution: an intramolecular (3 + 1) G-quadruplex scaffold. *J. Am. Chem. Soc.*, **128**, 9963–9970.
5. Dai,J., Punchihewa,C., Ambrus,A., Chen,D., Jones,R.A. and Yang,D. (2007) Structure of the intramolecular human telomeric G-quadruplex in potassium solution: a novel adenine triple formation. *Nucleic Acids Res.*, **35**, 2440–2450.
6. Phan,A.T., Kuryavyi,V., Luu,K.N. and Patel,D.J. (2007) Structure of two intramolecular G-quadruplexes formed by natural human telomere sequences in K+ solution. *Nucleic Acids Res.*, **35**, 6517–6525.
7. Dai,J., Carver,M., Punchihewa,C., Jones,R.A. and Yang,D. (2007) Structure of the hybrid-2 type intramolecular human telomeric G-quadruplex in K+ solution: insights into structure polymorphism of the human telomeric sequence. *Nucleic. Acids Res.*, **35**, 4927–4940.
8. Lim,K.W., Ng,V.C.M., Martín-Pintado,N., Heddi,B. and Phan,A.T. (2013) Structure of the human telomere in Na+ solution: an antiparallel (2+2) G-quadruplex scaffold reveals additional diversity. *Nucleic Acids Res.*, **41**, 10556–10562.
9. Lim,K.W., Amrane,S., Bouaziz,S., Xu,W., Mu,Y., Patel,D.J., Luu,K.N. and Phan,A.T. (2009) Structure of the human telomere in K+ solution: a stable basket-type G-quadruplex with only two G-tetrad layers. *J. Am. Chem. Soc.*, **131**, 4301–4309.
10. Zhang,Z., Dai,J., Veliath,E., Jones,R.A. and Yang,D. (2010) Structure of a two-G-tetrad intramolecular G-quadruplex formed by a variant human telomeric sequence in K+ solution: insights into the interconversion of human telomeric G-quadruplex structures. *Nucleic Acids Res.*, **38**, 1009–1021.
11. Galer, P., Wang, B., Šket, P., Plavec, L. (2016) Reversible pH Switch of Two-Quartet G-Quadruplexes Formed by Human Telomere. *Angewandte Chemie* **55**, 1993-1997.
12. Phan, A.T., Luu, K.N., Patel, D.J. (2006) Different loop arrangements of intramolecular human telomeric (3+1) G-quadruplex in K solution. *Nucleic Acids Res*. **34**, 5715-19.
13. Babinsky, M., Fiala, R., Kejnovska, I., Bednarova, K., Marek, R., Sagi, J., Sklenar, V., Vorlickova, M. (2014) Loss of loop adenines alters human telomere d[AG3(TTAG3)3] quadruplex folding. *Nucleic Acids Res.* **42**, 14031-14041.